

**Simultaneous  
Observations with  
Three FTSs**

D. Wunch et al.

# Simultaneous ground-based observations of O<sub>3</sub>, HCl, N<sub>2</sub>O, and CH<sub>4</sub> over Toronto, Canada by three Fourier transform spectrometers with different resolutions

D. Wunch<sup>1</sup>, J. R. Taylor<sup>1</sup>, D. Fu<sup>2</sup>, P. Bernath<sup>2,3</sup>, J. R. Drummond<sup>1,4</sup>, C. Midwinter<sup>1</sup>, K. Strong<sup>1</sup>, and K. A. Walker<sup>1,2</sup>

<sup>1</sup>Department of Physics, University of Toronto, Toronto, ON, M5S 1A7, Canada

<sup>2</sup>Department of Chemistry, University of Waterloo, Waterloo, ON, N2L 3G1, Canada

<sup>3</sup>Department of Chemistry, University of York, Heslington, York, YO10 5DD, UK

<sup>4</sup>Department of Physics and Atmospheric Science, Dalhousie University, Halifax, NS, B3H 3J5, Canada

Received: 19 September 2006 – Accepted: 19 October 2006 – Published: 26 October 2006

Correspondence to: D. Wunch (debra@atmosp.physics.utoronto.ca)

Title Page

Abstract

Introduction

Conclusions

References

Tables

Figures

◀

▶

◀

▶

Back

Close

Full Screen / Esc

Printer-friendly Version

Interactive Discussion

## Abstract

An intercomparison of three Fourier transform spectrometers (FTSs) with significantly different resolutions is presented. The highest-resolution instrument has a maximum optical path difference of 250 cm, and the two lower-resolution instruments have maximum optical path differences of 50 cm and 25 cm. The results indicate that the two lower-resolution instruments can retrieve total column amounts of O<sub>3</sub>, HCl, N<sub>2</sub>O and CH<sub>4</sub> using the SFIT2 retrieval code with percent differences from the high-resolution instrument generally better than 3%, with respect to the high-resolution FTS. Total column amounts of the stratospheric species (O<sub>3</sub> and HCl) have larger differences than those of the tropospheric species (N<sub>2</sub>O and CH<sub>4</sub>). Instrument line shape (ILS) information is found to be of critical importance when retrieving total columns of stratospheric gases from the lower-resolution instruments. Including the ILS information in the retrievals significantly reduces the difference in total column amounts between the three instruments. The remaining errors for stratospheric species total column amounts can be attributed to the lower sensitivity of the lower-resolution FTSs to the stratosphere.

## 1 Introduction

Ground-based measurements of infrared solar absorption by atmospheric trace gases using Fourier transform spectrometers (FTSs), have led to many important advances in our understanding of the atmosphere. This study presents an investigation of the differences in retrieved total column amounts of trace gases by three instruments of differing resolution. Previous intercomparisons of ground-based FTS observations have mainly focused upon the agreement of the retrieved quantities with instruments of similar resolution (Paton-Walsh et al., 1997; Goldman et al., 1999; Meier et al., 2005; Griffith et al., 2003) based on different analysis techniques (Goldman et al., 1999; Hase et al., 2004), or addressed how the influence of individual instrument performance impacts the retrieved vertical column concentrations (Meier et al., 2005; Griffith et al., 2003; Goldman

## Simultaneous Observations with Three FTSs

D. Wunch et al.

Title Page

Abstract

Introduction

Conclusions

References

Tables

Figures

◀

▶

◀

▶

Back

Close

Full Screen / Esc

Printer-friendly Version

Interactive Discussion

et al., 1999). Paton-Walsh et al. (1997) compared two instruments operating at a  $0.005 \text{ cm}^{-1}$  resolution for retrieving total columns of HCl,  $\text{N}_2\text{O}$  and  $\text{HNO}_3$ , and at  $0.07 \text{ cm}^{-1}$  for retrieving HF columns. Goldman et al. (1999) compared  $\text{N}_2$ , HF, HCl,  $\text{CH}_4$ ,  $\text{O}_3$ ,  $\text{N}_2\text{O}$ ,  $\text{HNO}_3$  and  $\text{CO}_2$  total columns measured by four FTSs at 50 cm maximum optical path difference (OPD). Meier et al. (2005) compared total columns of HCl, HF,  $\text{N}_2\text{O}$ ,  $\text{HNO}_3$ ,  $\text{CH}_4$ ,  $\text{O}_3$ ,  $\text{CO}_2$  and  $\text{N}_2$  from two high-resolution instruments (the maximum OPD used is unspecified in the paper). Griffith et al. (2003) compared total columns of  $\text{N}_2\text{O}$ ,  $\text{N}_2$ ,  $\text{CH}_4$ ,  $\text{O}_3$ , HCl,  $\text{HNO}_3$  and HF with two FTSs operating both at 180 cm maximum OPD (for all molecules except HF) and at 150 cm maximum OPD (for HF). There are no comparisons, to our knowledge, that look at total columns produced by data from FTS instruments with significantly different resolutions.

In this study, we compare two FTS instruments that are used both on balloon platforms and on the ground to one that is used solely for ground-based measurements. The two balloon-based and ground-based instruments, called the University of Toronto's Fourier Transform Spectrometer (U of T FTS) and the Portable Atmospheric Research Interferometric Spectrometer for the Infrared (PARIS-IR), have spectral resolutions corresponding to 50 cm and 25 cm OPD, respectively. Both instruments have participated in the 2004 Middle Atmosphere Nitrogen TRend Assessment (MANTRA) high-altitude balloon campaign (Strong et al., 2005). The ground-based FTS, called the Toronto Atmospheric Observatory Fourier Transform Spectrometer (TAO-FTS), has a maximum OPD of 250 cm, and is a complementary instrument of the Network for the Detection of Atmospheric Composition Change (NDACC—formerly the Network for the Detection of Stratospheric Change (NDSC) Kurylo and Zander, 2000).

The goals of this intercomparison are to retrieve total column amounts of ozone ( $\text{O}_3$ ), hydrogen chloride (HCl), nitrous oxide ( $\text{N}_2\text{O}$ ), and methane ( $\text{CH}_4$ ) from the data recorded simultaneously by these three instruments, to determine which retrieval parameters most affect and improve the retrieved column amounts for the lower-resolution instruments, and to determine the causes of any remaining discrepancies.

---

## Simultaneous Observations with Three FTSs

D. Wunch et al.

---

[Title Page](#)[Abstract](#)[Introduction](#)[Conclusions](#)[References](#)[Tables](#)[Figures](#)[◀](#)[▶](#)[◀](#)[▶](#)[Back](#)[Close](#)[Full Screen / Esc](#)[Printer-friendly Version](#)[Interactive Discussion](#)

## 2 Instruments

### 2.1 TAO FTS

The Toronto Atmospheric Observatory (43°40' N, 79°24' W, 174.0 m) was established in 2001 with the installation of a high-resolution, DA8 model infrared Fourier transform spectrometer manufactured by ABB Bomem Inc. The TAO-FTS was designated a complementary instrument of the NDACC in March, 2004. Since then, the TAO-FTS has taken part in both satellite validation activities (Mahieu et al., 2005; Dils et al., 2006) and scientific process studies (Wiacek et al., 2006).

The optical design of the TAO-FTS instrument consists of a vertically oriented, linear Michelson interferometer that records single-sided interferograms with a maximum optical path difference of 250 cm (Wiacek et al., in press). The modulation efficiency and phase error are shown in the left-most panels of Fig. 1. Infrared solar absorption spectra are nominally recorded on indium antimonide (InSb) and mercury cadmium telluride (MCT) detectors using a potassium bromide (KBr) beamsplitter to cover the spectral region from 750 to 4400 cm<sup>-1</sup> (2.3–13.3 μm). The external optical components include a dedicated elevation-azimuth tracker (manufactured by AIM Controls Inc.) which actively tracks direct solar radiation throughout the day, as well as several flat mirrors and a collimating mirror used to direct the radiation into the interferometer.

Observations are usually taken by sequencing through six different narrow-band optical interference filters, all of which are widely used within the NDACC InfraRed Working Group (IRWG). For the purposes of this campaign, only one of these filters is used with the InSb detector, reducing the spectral range to 2400–3100 cm<sup>-1</sup> (3.2–4.2 μm). This range is ideal for this study because it contains signatures of the molecules of interest in a spectral region that is measured by the other two instruments. To attain a sufficiently high signal-to-noise ratio, each spectrum is produced by co-adding four, 250-cm optical path difference scans, resulting in one interferogram attained over a period of approximately 20 min. Each interferogram is Fourier transformed into a spectrum using

## Simultaneous Observations with Three FTSs

D. Wunch et al.

Title Page

Abstract

Introduction

Conclusions

References

Tables

Figures

◀

▶

◀

▶

Back

Close

Full Screen / Esc

Printer-friendly Version

Interactive Discussion

a boxcar apodization scheme (i.e. unapodized).

## 2.2 U of T FTS

The University of Toronto's Fourier Transform Spectrometer is an ABB Bomem DA5 instrument that has a 50-cm maximum optical path difference, and records single-sided interferograms along a linear mirror path (Wunch et al., 2006). The instrument measures simultaneously on InSb and MCT detectors. Both detectors are photovoltaic in order to ensure linearity. The U of T FTS has a spectral range spanning 1200–5000  $\text{cm}^{-1}$  (2–8.3  $\mu\text{m}$ ) that is constrained by the detectors, the calcium fluoride ( $\text{CaF}_2$ ) beamsplitter and a germanium solar filter.

The instrument has had new electronics and software installed so that it can be used both on high-altitude balloon platforms and on the ground. The U of T FTS has also been fitted with a sun tracker with a small tracking range ( $\pm 10^\circ$  in both elevation and azimuth). The tracker is used for this intercomparison to easily couple the solar beam from the TAO sun tracker into the U of T FTS.

The instrument lineshape of the U of T FTS is imperfect (Fig. 1, middle panels), due to a hard landing after the MANTRA 2004 balloon flight, reducing the effective resolution to near  $0.03 \text{ cm}^{-1}$  and causing a significant phase error. To make the best use of the data, interferograms from the U of T FTS are apodized with a triangular function. This improves the signal-to-noise ratio of the data without significant further loss of resolution.

For the purpose of this intercomparison campaign, only data from the MCT detector are shown as there were ongoing InSb detector mount changes. The ranges of the two detectors overlap in all regions of interest for this study.

## 2.3 PARIS-IR

The Atmospheric Chemistry Experiment Fourier Transform Spectrometer (ACE-FTS) is the primary instrument on the Canadian scientific satellite mission SCISAT-1, which

### Simultaneous Observations with Three FTSs

D. Wunch et al.

Title Page

Abstract

Introduction

Conclusions

References

Tables

Figures

◀

▶

◀

▶

Back

Close

Full Screen / Esc

Printer-friendly Version

Interactive Discussion

---

**Simultaneous  
Observations with  
Three FTSs**D. Wunch et al.

---

Title Page

Abstract

Introduction

Conclusions

References

Tables

Figures

◀

▶

◀

▶

Back

Close

Full Screen / Esc

Printer-friendly Version

Interactive Discussion

was launched by NASA on 12 August 2003 (Bernath et al., 2005). The Portable Atmospheric Research Interferometric Spectrometer for the Infrared is a new, compact, portable FTS built by ABB Bomem for the Waterloo Atmospheric Observatory (43° 28' N, 80°33' W, 319.0 m) (Fu et al., 2006). PARIS-IR was primarily constructed from spare flight components that were manufactured for the ACE-FTS and consequently has a very similar optical design, producing double-sided interferograms with the same maximum OPD (25 cm) and spectral range (750–4400 cm<sup>-1</sup>). The sandwich detectors are composed of a photovoltaic InSb detector and a photoconductive MCT detector, which is corrected for detector nonlinearity. The data presented here, however, are only from the InSb detector. To obtain a sufficiently long optical path difference within a compact volume, ABB Bomem used a “double pendulum” interferometer and also used an “entrance mirror” to pass radiation through the interferometer twice. In addition to the MANTRA campaign in August 2004, PARIS-IR has participated in three ground-based ACE validation campaigns in the Canadian high Arctic at Eureka, Nunavut (Kerzenmacher et al., 2005). Currently, the instrument is regularly operated at the Waterloo Atmospheric Observatory (WAO) for recording ground-based atmospheric absorption spectra. The PARIS-IR modulation efficiency and phase error are shown in the right-most panels of Fig. 1. The PARIS-IR interferograms are unapodized.

### 3 Observation strategy and analysis method

The observation strategy for the campaign was constructed to focus on the effects of the instrument resolution on the retrieved column amounts. This was achieved by measuring simultaneously from the same location, in the same spectral range, and using similar retrieval methods with identical a priori information, line parameters and forward model. All three instruments were located at TAO for the duration of the campaign. The data presented here were recorded on 24 August, 26 August, 1 September and 2 September 2005, with at least 14 spectra recorded by the TAO-FTS on each day.

Retrievals for all three instruments were executed using SFIT2 (v.3.82beta3) (Rins-

land et al., 1998; Pougatchev et al., 1995) and the same input parameters. SFIT2 is a retrieval algorithm based on the SFIT1 algorithm (Rinsland et al., 1982) that employs the optimal estimation method (OEM) of Rodgers (2000). This algorithm retrieves a state vector that consists of the primary trace gas volume mixing ratio (VMR) vertical profile represented on an altitude grid, interfering species fit from scaled VMR profiles, and other ancillary fitting parameters.

The model atmospheres were generated by FSCATM (Gallery et al., 1983; Meier et al., 2004), a nonlinear forward model that uses an a priori state estimate, pressure profiles, and temperature profiles to perform refractive ray tracing and a calculation of the air mass distribution for a model atmosphere. The a priori state estimates of VMR profiles and columns were constructed from a combination of climatological estimates from the HALogen Occultation Experiment (HALOE) v.19 satellite data (Russell et al., 1994) and mid-latitude daytime 2001 Michelson Interferometer for Passive Atmospheric Sounding (MIPAS) reference profiles (Carli et al., 2004). Details of the a priori construction can be found in Wiacek et al. (in press) and in Sect. 4.1 of Wiacek (2006). Pressure and temperature profiles were obtained from National Centers for Environmental Prediction/National Center for Atmospheric Research analyses provided by the NASA Goddard Space Flight Centre automailer (Schoeberl et al.). The High resolution TRANsmiission molecular absorption database (HITRAN) 2004 (Rothman et al., 2005) was used for the spectroscopic line parameters.

To measure the same atmospheric path simultaneously with all three instruments, two small pick-off mirrors were placed in the TAO suntracker's solar beam to deflect a portion of the light into the U of T FTS and PARIS-IR (see Fig. 2). Every attempt was made to ensure that the TAO FTS incurred a minimal loss of signal, and that its signal-to-noise ratio was reduced by less than 10%. The TAO instrument, as described in Sect. 2.1, requires 5 min to record one interferogram and ~20 min for a spectrum derived from 4 co-added interferograms. To further ensure simultaneity, the U of T FTS and PARIS-IR co-added individual spectra that were recorded during the 20-min interval required to produce one TAO-FTS spectrum. The PARIS-IR instrument measures

---

## Simultaneous Observations with Three FTSs

D. Wunch et al.

---

Title Page

Abstract

Introduction

Conclusions

References

Tables

Figures

◀

▶

◀

▶

Back

Close

Full Screen / Esc

Printer-friendly Version

Interactive Discussion

the largest number of spectra per unit time, with a 20-s scan time, whereas the U of T FTS measures one interferogram in 50 s. Table 1 summarizes the instrument details.

The three FTS instruments measured solar absorption by O<sub>3</sub>, CH<sub>4</sub>, HCl, and N<sub>2</sub>O in overlapping regions of their spectral ranges. The five microwindows used in this campaign are listed in Table 2. Two microwindows for ozone (near 3040 cm<sup>-1</sup> and 2775 cm<sup>-1</sup>) were chosen because they yielded the highest degrees of freedom for signal for the lower resolution instruments in the spectral range considered, compared with the more commonly used 3045 cm<sup>-1</sup> microwindow (e.g., Goldman et al., 1999, Griffith et al., 2003). It should be noted that the best ozone retrievals for the PARIS-IR instrument come from the 1000 cm<sup>-1</sup> band, but in the interest of consistency, retrievals of ozone are considered only in the spectral ranges measured by all three instruments.

The only difference between the three retrieval methods is that the PARIS-IR retrievals were performed on a 29-layer grid, whereas the TAO and U of T FTS retrievals were performed on a 38-layer grid. As discussed in Sect. 3.4 below, this made only a small difference in the resulting column amounts.

By eliminating atmospheric condition differences between measurements, eliminating differences in line parameter characterization and minimizing the differences in the retrieval methods, the bulk of the discrepancies can now be attributed to differences in instrument resolution.

### 3.1 Instrument Line Shape

The importance of considering the influence of an individual instrument line shape (ILS) for ground-based comparisons has been previously addressed (Griffith et al., 2003) and is particularly important in this case because of the pronounced differences in the resolution of the three instruments. Information about the ILS can be incorporated in the forward model by using tabular inputs to describe the effective apodization and phase error as a function of OPD, or by using polynomial coefficients to describe effective apodization parameters (EAP) and phase error parameters (PHS).

For either of these two cases, a measurement made by each of the three spec-

## Simultaneous Observations with Three FTSs

D. Wunch et al.

Title Page

Abstract

Introduction

Conclusions

References

Tables

Figures

◀

▶

◀

▶

Back

Close

Full Screen / Esc

Printer-friendly Version

Interactive Discussion

trometers must be analysed to determine the values of these empirical parameters. This can be done under controlled conditions using calibrated gas cells (Coffey et al., 1998) and an independent retrieval algorithm designed to determine ILS information. We used the LINEFIT code of Hase et al. (1999): version 9.0 for the U of T FTS and TAO-FTS and version 11.0 for the PARIS-IR. The U of T FTS and TAO-FTS measured blackbody radiation through an HBr cell to calculate the ILS, and PARIS-IR measured blackbody radiation through an N<sub>2</sub>O cell. LINEFIT produces tabular modulation efficiency and phase error results as a function of OPD, which, once the modulation efficiency values are converted to effective apodization values, can be used as inputs into SFIT2. Inherent in this technique is the assumption that the ILS measured under these controlled conditions is identical to the ILS throughout the duration of all atmospheric measurements. This may be largely true over a few months for ground-based measurements, however, it will not generally be true for balloon-based measurements, since temperatures change significantly between daytime and nighttime, and both the atmospheric temperature and pressure vary significantly between the ground and the float altitude. Both temperature and pressure can affect the instrument alignment and thus the ILS. Because of this, we may wish to calculate the ILS for each spectrum individually. Without a permanent gas cell in the optical path of each spectrometer during solar measurements (which none of these instruments possess), a method for retrieving ILS information from the solar spectrum itself is necessary.

SFIT2 provides a solution for this with a parameter that allows for EAP and PHS polynomial coefficients to be retrieved as part of the state vector. We chose to retrieve third-order polynomial coefficients for both the PHS and EAP parameters. In the sections that follow, when we discuss “tabular” ILS information, we are referring to LINEFIT results used as an input to SFIT2. Retrievals using the LINEFIT tabular inputs will be labeled “ILS input”. When we discuss “polynomial” ILS information, we are referring to the PHS and EAP parameters retrieved from SFIT2. Retrievals that contain PHS and EAP parameters from SFIT2 will be referred to as “PHS/EAP retrieved”. When neither the LINEFIT tabular nor SFIT2 polynomial ILS information is included in a retrieval, we

---

## Simultaneous Observations with Three FTSs

D. Wunch et al.

---

[Title Page](#)[Abstract](#)[Introduction](#)[Conclusions](#)[References](#)[Tables](#)[Figures](#)[◀](#)[▶](#)[◀](#)[▶](#)[Back](#)[Close](#)[Full Screen / Esc](#)[Printer-friendly Version](#)[Interactive Discussion](#)

will call this our “standard retrieval”. The TAO-FTS regularly retrieves a simple phase parameter (SPHS) from SFIT2. SPHS is a single-parameter description of the asymmetry of a spectral line, and is included in all three retrieval types (ILS input, PHS/EAP retrieved and the standard retrieval).

5 The U of T FTS and PARIS-IR instruments retrieve PHS and EAP information somewhat differently. The method employed for the U of T FTS spectra retrieves third-order polynomial PHS and EAP parameters from the same microwindow as the retrieved species (that is, only one retrieval is necessary for each molecule). The method employed for the PARIS-IR data, however, retrieves third-order polynomial PHS and EAP  
10 parameters from a very broad N<sub>2</sub>O band in the 2806.1–2808.1 cm<sup>-1</sup> microwindow, using a priori values from LINEFIT, and fixes the daily mean of those values for all spectra when retrieving the other species. (EAP and PHS parameters can also be retrieved from each spectrum, but for reasons of efficiency, we use daily means, here.) This method was attempted for the U of T FTS data with less success than directly  
15 retrieving the parameters from the same microwindow. We believe that the success of the second, dedicated microwindow for retrieving the ILS parameters for the PARIS-IR instrument may be in part due to the lower degrees of freedom for signal retrieved from the PARIS-IR spectra. Instead of retrieving profile, PHS and EAP information from a given microwindow with limited information, we are providing extra ILS information from  
20 the same spectrum, but in a different microwindow.

### 3.2 Effects of resolution

To simulate the effect of resolution on total column amounts, an ensemble of 16 spectra was simulated for the same atmospheric conditions for each of 12 cm, 25 cm, 50 cm, 100 cm, 150 cm, 200 cm and 250 cm maximum OPD. The signal-to-noise ratio was set  
25 to 250 for each spectrum to simulate a typical measurement noise value, and all four molecules were retrieved using the same a priori values as our data from 1 September. Identical phase and effective apodization errors were applied to each spectrum, with values similar to the TAO instrument (Fig. 1, left-most panels). All results below are

---

## Simultaneous Observations with Three FTSs

D. Wunch et al.

---

Title Page

Abstract

Introduction

Conclusions

References

Tables

Figures

◀

▶

◀

▶

Back

Close

Full Screen / Esc

Printer-friendly Version

Interactive Discussion

consistent with an ensemble of measured spectra from a single day of TAO measurements for which the interferograms were truncated to the same set of OPD values.

In Figs. 3–7, the retrieved column amounts of O<sub>3</sub>, HCl, N<sub>2</sub>O and CH<sub>4</sub> are shown as a function of the optical path difference. The figures show the mean column amounts with the 2σ standard deviation of the ensemble for two sets of retrievals: one that retrieves third-order polynomial coefficients for the PHS and EAP functions (“PHS/EAP retrieved”) from the microwindow itself, and one that does not retrieve coefficients (our “standard retrieval”). The a priori column value and the “truth” are plotted for reference. The truth in this case is the column amount used to create the model spectra.

For ozone in the 3040 cm<sup>-1</sup> microwindow (Fig. 3), there is less than 0.67% difference in column amounts retrieved at 250 cm OPD between the standard and PHS/EAP retrieved cases, with the standard retrieval being essentially indistinguishable from the truth (~0.07% larger). The PHS/EAP retrieved case changes less than the standard retrieval between the different OPD values, and retrieves columns that are closer to the truth at the lowest OPDs (except for 25 cm). The results are within 1% of the truth for all OPDs for the PHS/EAP retrieved case and differ by more than 1% from the truth for the 50 cm OPD and 12 cm OPD standard retrieval. We would expect, then, good results from the lower resolution instruments using this microwindow if they retrieve PHS and EAP parameters.

Ozone retrieved from the 2775 cm<sup>-1</sup> microwindow is shown in Fig. 4. At 250 cm OPD, the columns differ by less than 0.06% from the truth, obtained by either the standard retrieval or the PHS/EAP retrieved case. The column average for the standard retrieval begins to decrease significantly below 100 cm OPD with the column mean over the ensemble differing by <7% from the truth at 50 cm OPD. The PHS/EAP retrieved case has less than 1% difference down to 25 cm OPD, whereas the standard retrieval gives a mean that is 19.4% smaller than the true value at 25 cm OPD. The simulated retrievals did not converge for the PHS/EAP retrieval at 12 cm OPD, so are not plotted here. We may expect, then, that we should get good results for ozone for the lower-resolution instruments if they retrieve PHS/EAP parameters.

---

## Simultaneous Observations with Three FTs

D. Wunch et al.

---

[Title Page](#)[Abstract](#)[Introduction](#)[Conclusions](#)[References](#)[Tables](#)[Figures](#)[⏪](#)[⏩](#)[◀](#)[▶](#)[Back](#)[Close](#)[Full Screen / Esc](#)[Printer-friendly Version](#)[Interactive Discussion](#)

For HCl (Fig. 5), the difference in columns retrieved between the standard retrieval at 250 cm OPD and the truth is 0.27% and between the PHS/EAP retrieved case at 250 cm OPD and the truth is 0.36%. The column amounts are within 1% of the truth until 50 cm OPD for the standard retrieval, and 25 cm OPD for the PHS/EAP retrieved case. At and below 50 cm OPD, the percent difference from the truth increases in both cases, with the PHS/EAP retrieved case showing significantly better agreement than the standard case. We would expect, then, reasonable agreement for HCl for the lower resolution instruments if PHS and EAP parameters are retrieved.

For N<sub>2</sub>O (Fig. 6), the difference between the columns retrieved with the standard retrieval at 250 cm OPD and the truth is ~0.5%, and the difference in columns between the PHS/EAP retrieval at 250 cm OPD and the truth is ~0.02%. The N<sub>2</sub>O columns show good agreement with the truth (<1%) for all OPDs for the PHS/EAP retrieved case, and good agreement with the truth for all OPDs at or larger than 100 cm for the standard retrieval. Below 100 cm OPD, the standard retrieval stays within ~2% of the truth, and does not have the drastic decrease that the stratospheric species show. We would expect, then, that all three instruments would have good agreement for N<sub>2</sub>O if they perform either retrieval, but better results may be obtained from the lower resolution instruments if they retrieve PHS and EAP parameters.

For CH<sub>4</sub> (Fig. 7), the difference between columns retrieved using the standard retrieval at 250 cm OPD and the truth is ~0.34%, and the difference in columns between the PHS/EAP retrieval at 250 cm OPD and the truth is ~0.22%. The CH<sub>4</sub> columns show good agreement with the truth (<1%) for all OPDs for the PHS/EAP retrieved case, except for 100 cm OPD, where the percent difference from the truth is ~1.05%. There is good agreement with the truth for all OPDs for the standard retrieval, except for 25 cm OPD where the difference is ~2.35%. Again, as for N<sub>2</sub>O, the two retrieval cases stay within ~2.5% of the truth, and do not show a significant decrease at smaller OPD. We would expect, then, that all three instruments would have good agreement for CH<sub>4</sub> if they perform either retrieval.

**Simultaneous  
Observations with  
Three FTs**

D. Wunch et al.

Title Page

Abstract

Introduction

Conclusions

References

Tables

Figures

◀

▶

◀

▶

Back

Close

Full Screen / Esc

Printer-friendly Version

Interactive Discussion

### 3.3 Comparison of columns using PHS/EAP and LINEFIT

It has been noted by Griffith et al. (2003) that stratospheric species ( $O_3$  and HCl), which have narrow absorption lines, are highly sensitive to ILS distortions, while pressure-broadened tropospheric species ( $N_2O$  and  $CH_4$ ) are less sensitive to them. We have confirmed this and have investigated column differences obtained when retrieving the EAP and PHS with SFIT2 as compared with columns retrieved when using LINEFIT results as inputs to SFIT2. The first test run retrieved PHS and EAP parameters (“PHS/EAP retrieved”) using the microwindow itself in the U of T FTS case, and the broad  $N_2O$  microwindow in the PARIS-IR case. The second test run used tabular LINEFIT inputs (“ILS input”) obtained from a gas cell measurement. The third test run used only SPHS ILS information (“standard retrieval”). No significant differences in retrieved column amounts between the three ILS cases are seen for the TAO-FTS. Therefore, for our purposes, TAO-FTS data is considered to be closest to the truth.

For the U of T FTS, the best ozone column comparisons were from using the ILS input run (Fig. 8). For  $O_3$  in the  $3040\text{ cm}^{-1}$  microwindow, the ILS input run is only slightly closer to the TAO-FTS mean values (by  $\sim 0.4\%$ ) than the PHS/EAP retrieval and both are more than 20% higher than the values from the standard run. The spectral fits from the PHS/EAP retrieved and ILS input cases also show smaller residuals (see Fig. 9). The PARIS-IR results are similar—retrieving PHS/EAP parameters improved the agreement in the column amounts by  $\sim 8\%$  over the standard retrieval (Fig. 8) and the spectral fits are better for the PHS/EAP retrieval and the ILS input cases than for the standard retrieval. Similar results are found for ozone in the  $2775\text{ cm}^{-1}$  microwindow (Fig. 8).

The sensitivity of the U of T FTS HCl retrieval to the ILS is also high, as illustrated in Figs. 8 and 10, with the PHS/EAP retrieved run being closer (by  $\sim 1\%$ ) to the TAO-FTS columns than the ILS input run. The difference in HCl columns between the PHS/EAP retrieved and standard retrievals for the PARIS-IR instrument is  $\sim 2\%$ , with the standard retrieval mean slightly closer to the TAO-FTS retrieved values (Fig. 8). Residuals

## Simultaneous Observations with Three FTSs

D. Wunch et al.

Title Page

Abstract

Introduction

Conclusions

References

Tables

Figures

◀

▶

◀

▶

Back

Close

Full Screen / Esc

Printer-friendly Version

Interactive Discussion

from the spectral fits for both the U of T FTS and PARIS-IR show, like in O<sub>3</sub>, that the PHS/EAP retrieval and ILS input cases are smaller than for the standard retrieval.

The U of T FTS N<sub>2</sub>O retrieval is much less sensitive to the ILS, as illustrated in Figs. 8 and 11, although the PHS/EAP retrieved values are closer to the TAO-FTS values than those from the standard retrieval. The sensitivity of the PARIS-IR retrieval to the ILS in the PHS/EAP retrieved case is also quite low. There is only a ~0.4% difference between the PHS/EAP and standard cases (Fig. 8). The residuals from the spectral fits for both the U of T FTS and PARIS-IR instruments show only slightly better results for the PHS/EAP retrieval and ILS input cases than for the standard retrieval.

The sensitivity of the U of T FTS CH<sub>4</sub> retrievals to the ILS is also lower than that found for O<sub>3</sub> and HCl, as illustrated in Figs. 8 and 12. (The other two spectral microwindows for CH<sub>4</sub> have similar residuals and are not shown.) Retrieving the PHS and EAP parameters for the U of T FTS data produces poorer comparisons with the TAO-FTS data, because it induces spurious oscillations in the profile. There is systematic structure in the residuals from the CH<sub>4</sub> spectral fits for all three retrieval cases for both PARIS-IR and the U of T FTS. The TAO-FTS residuals also show systematic structure, pointing to a possible problem with the methane spectroscopy. The sensitivity of the PARIS-IR retrieval of CH<sub>4</sub> to the ILS is very low, with only ~0.6% difference between the PHS/EAP retrieved and standard retrievals (Fig. 8).

The U of T FTS ILS is much poorer than that of PARIS-IR (compare the central and right panels in Fig. 1). Accordingly, the difference in total columns retrieved by the U of T FTS for the PHS/EAP retrieved case and the standard retrieval will be exaggerated for the stratospheric species, which are most sensitive to ILS distortions. Nevertheless, using either the PHS/EAP retrieved or the ILS input cases for both lower-resolution instruments results in reasonable agreement with the TAO-FTS.

Using the results from this section, for what follows, we use the PHS/EAP retrieved case to compute columns of O<sub>3</sub>, HCl and N<sub>2</sub>O for the U of T FTS. The standard retrieval is used for CH<sub>4</sub>. For PARIS-IR, the PHS/EAP retrieved case is used for O<sub>3</sub> and HCl, and the standard retrieval is used for N<sub>2</sub>O and CH<sub>4</sub>. Since the TAO-FTS line shape is

---

## Simultaneous Observations with Three FTSs

D. Wunch et al.

---

[Title Page](#)[Abstract](#)[Introduction](#)[Conclusions](#)[References](#)[Tables](#)[Figures](#)[⏪](#)[⏩](#)[◀](#)[▶](#)[Back](#)[Close](#)[Full Screen / Esc](#)[Printer-friendly Version](#)[Interactive Discussion](#)

significantly narrower than both the stratospheric and tropospheric absorption lines, it is much less sensitive to instrument line shape distortions, and the standard retrieval is always used. Retrieving the PHS and EAP parameters for the TAO-FTS makes only small changes (<1%) in total columns retrieved. Table 3 summarizes the retrieval parameters for these results.

### 3.4 Number of grid levels

The PARIS-IR analysis retrieves profiles on a 29-layer vertical grid, whereas the TAO-FTS and U of T FTS retrieve profiles on a 38-layer grid. The 29-layer vertical grid was chosen for the PARIS-IR retrievals to reduce the size of the state vector, in order to compensate for the lower resolution of the measurements. To ensure that the number of grid levels does not significantly affect the results in this intercomparison, we compared column amounts retrieved for a single day of measurements from the PARIS-IR instrument both on a 29-layer grid and a 38-layer grid.

For N<sub>2</sub>O and CH<sub>4</sub>, there was no noticeable difference (<0.1%) in column amounts retrieved from the PARIS-IR data between retrieving on a 29-layer grid and a 38-layer grid. For ozone in the 3040 cm<sup>-1</sup> microwindow, the 38-layer results were ~0.2% lower than the 29-layer results. For ozone in the 2775 cm<sup>-1</sup> microwindow, the 38-layer results were ~0.6% higher than the 29-layer results. For HCl, the 38-layer results were ~0.4% higher than the 29-layer results. The number of grid levels, therefore, is not a significant influence on the results in this comparison.

## 4 Results

These measurements took place during a nine-day period in late August and early September, 2005. Because of the relatively stable chemistry and dynamics of the atmosphere during that time, we do not expect any significant trends in column amounts of any of these molecules. Total column amounts are, consequently, plotted as a func-

### Simultaneous Observations with Three FTSs

D. Wunch et al.

Title Page

Abstract

Introduction

Conclusions

References

Tables

Figures

◀

▶

◀

▶

Back

Close

Full Screen / Esc

Printer-friendly Version

Interactive Discussion

## Simultaneous Observations with Three FTs

D. Wunch et al.

Title Page

Abstract

Introduction

Conclusions

References

Tables

Figures

◀

▶

◀

▶

Back

Close

Full Screen / Esc

Printer-friendly Version

Interactive Discussion

tion of solar zenith angle (SZA) in Figs. 13–17. The total column errors in the figures consist of the interference error (Rodgers and Connor, 2003), retrieval noise, and smoothing error (Rodgers, 2000) added in quadrature. There is a clear discrepancy (most pronounced for CH<sub>4</sub>) between the column amounts at angles larger than and smaller than 40 degrees SZA. We believe that this may be due to suntracker error near solar noon, and so we do not include the data taken at angles less than 40 degrees in our means. The total column means, as given in Table 4, show that the lower-resolution instruments are capable of providing column amounts of all species to within ~3% of the TAO-FTS. The agreement is worse than that found in the Meier et al. (2005) paper (also listed in the table) with two, similarly high-resolution instruments, and so our results may give an upper bound on the ability to measure total column amounts of these species by lower-resolution instruments.

Methane shows larger errors than might be expected from a tropospheric species retrieval, with significantly different retrieved columns obtained from the three FTs. This is possibly caused by the more poorly understood spectroscopy of methane, specifically the lack of accurate air-broadening coefficients and temperature dependencies, which has been noted by Rothman et al. (2005), Brown et al. (2003) and Worden et al. (2004).

A possibility for the differences in the stratospheric total column amounts is due to the instruments' column averaging kernels. In what follows, boldface capital variable names represent matrices, boldface lowercase italic variable names represent vectors and lightface italic variable names represent scalars. The OEM retrieved profile,  $\hat{x}$ , is a weighted average of the a priori profile,  $x_a$ , and the "truth,"  $x$ , weighted by the averaging kernel,  $\mathbf{A} = \partial \hat{x} / \partial x$  (Rodgers, 2000):

$$\hat{x} = \mathbf{A}x + (\mathbf{I} - \mathbf{A})x_a. \quad (1)$$

The retrieved total column,  $\hat{c}$ , is found by multiplying the retrieved profile by the atmospheric density or air mass,  $\rho$ :  $\hat{c} = \rho \hat{x}$ . This provides a total column averaging kernel,

$$\mathbf{a}_\rho,$$

$$\mathbf{a}_\rho = \rho \mathbf{A}. \quad (2)$$

Typically, the  $\mathbf{a}_\rho$  is normalized by the density (i.e.  $\mathbf{a}_\rho \rho_i^{-1}$ ) when plotted. However, we prefer the density-weighted version, since it more accurately illustrates at what altitude the retrieved column amount is sensitive. In Fig. 18, the density-weighted column averaging kernels,  $\mathbf{a}_\rho$ , are shown for each instrument (the normalized column averaging kernels are shown in Fig. 19 for reference). There are significant differences between them, with the PARIS-IR results showing the lowest sensitivity.

To test the sensitivity of the U of T FTS and PARIS-IR retrievals to the stratosphere, the averaging kernels were applied to a profile that was 20% larger than the a priori profile at each level and the column was computed using the air mass,  $\rho$ . That is, the profile and column estimates are

$$\hat{\mathbf{x}} = \mathbf{A}(1.2\mathbf{x}_a) + (\mathbf{I} - \mathbf{A})\mathbf{x}_a = (0.2\mathbf{A} + \mathbf{I})\mathbf{x}_a, \quad (3)$$

$$\hat{\mathbf{c}} = \rho(0.2\mathbf{A} + \mathbf{I})\mathbf{x}_a = (0.2\mathbf{a}_\rho + \rho)\mathbf{x}_a. \quad (4)$$

In this case, shown in Fig. 20, there are significant column differences between the TAO-FTS results and the U of T FTS and PARIS-IR results. The red lines indicate the a priori column and the green lines indicate the a priori column increased by 20% (the “truth”, here). Results with the a priori increased by a larger amount show larger differences between the retrieved columns and the truth.

For  $\text{O}_3$  in the  $3040 \text{ cm}^{-1}$  microwindow, the percent differences from the TAO-FTS are:  $-0.9\%$  for the U of T FTS and  $-1.8\%$  for PARIS-IR; for ozone in the  $2775 \text{ cm}^{-1}$  microwindow:  $-0.2\%$  for the U of T FTS and  $-6.7\%$  for PARIS-IR; for HCl:  $-1.4\%$  for the U of T FTS and  $-8.4\%$  for PARIS-IR; for  $\text{N}_2\text{O}$ :  $-0.01\%$  for the U of T FTS and  $-0.5\%$  for PARIS-IR; and for  $\text{CH}_4$ :  $-0.2\%$  for the U of T FTS and  $-0.6\%$  for PARIS-IR.

The stratospheric species clearly show larger differences as we have also seen in Table 4. The differences in the stratospheric species, therefore, can be partially attributed to the lower sensitivity of the lower-resolution instruments to the stratosphere and the

## Simultaneous Observations with Three FTSs

D. Wunch et al.

Title Page

Abstract

Introduction

Conclusions

References

Tables

Figures

◀

▶

◀

▶

Back

Close

Full Screen / Esc

Printer-friendly Version

Interactive Discussion

consequent increased reliance on the a priori in that region. It is therefore particularly important to choose appropriate microwindows and perform sufficient characterization of the lower-resolution instruments, to optimize the sensitivity.

## 5 Conclusions

5 Total column amounts of  $O_3$ , HCl,  $N_2O$  and  $CH_4$  were retrieved from PARIS-IR, the U of T FTS and the TAO-FTS. Measurements were averaged during coincident 20-min periods and the total column amounts retrieved from these averaged spectra were compared directly. The results, given in Figs. 13–17 and summarized in Table 4, show that the lower-resolution instruments can measure total columns of  $O_3$ ,  $CH_4$ , HCl and

10  $N_2O$  to within  $\sim 3\%$ , on average, of the truth (taken here as the results from the high-resolution TAO-FTS) from the ground. The largest errors are obtained for the stratospheric species, and these errors can be attributed to the averaging kernels of the lower-resolution instruments (Figs. 18–20). The errors from the methane retrievals are possibly due to uncertainties in the spectroscopy.

15 Retrieving ILS PHS and EAP parameters from SFIT2 significantly improves the column comparisons of the stratospheric species for the lower-resolution instruments (Fig. 8). The ILS information is less important for the pressure-broadened tropospheric species. Also, retrieving the SFIT2 PHS and EAP parameters as part of the state vector can replace the LINEFIT ILS information for balloon-based measurements when

20 retrieving the ILS from a gas cell is not feasible.

*Acknowledgements.* The authors wish to thank P. Fogal, K. Sung, N. Jones and F. Hase for helpful discussions, and F. Hase also for providing the LINEFIT code. We wish to thank M. Jensen, A. Wiacek, T. Kerzenmacher, O. Mikhailov, and K. MacQuarrie for their technical support and help with measurements. Funding for this work was provided by NSERC, CSA, CFCAS and ABB Bomem. TAO has been established with support from CFI, ORDCE, CRESTech, and the University of Toronto. Support at the University of Waterloo was provided by the NSERC-Bomem-CSA-MSc Industrial Research Chair in Fourier Transform Spec-

25

---

### Simultaneous Observations with Three FTSs

D. Wunch et al.

---

Title Page

Abstract

Introduction

Conclusions

References

Tables

Figures

◀

▶

◀

▶

Back

Close

Full Screen / Esc

Printer-friendly Version

Interactive Discussion

## References

- Bernath, P. F., McElroy, C. T., Abrams, M. C., Boone, C. D., Butler, M., Camy-Peyret, C., Carleer, M., Clerbaux, C., Coheur, P. F., Colin, R., DeCola, P., DeMazière, M., Drummond, J. R., Dufour, D., Evans, W. F. J., Fast, H., Fussen, D., Gilbert, K., Jennings, D. E., Llewellyn, E. J., Lowe, R. P., Mahieu, E., McConnel, J. C., McHugh, M., McLeod, S. D., Michaud, R., Midwinter, C., Nassar, R., Nichitiu, F., Nowlan, C., Rinsland, C. P., Rochon, Y. J., Rowlands, N., Semeniuk, K., Simon, P., Skelton, R., Sloan, J. J., Soucy, M. A., Strong, K., Tremblay, P., Turnbull, D., Walker, K. A., Walkty, I., Wardle, D. A., Wehrle, V., Zander, R., and Zou, J.: Atmospheric Chemistry Experiment (ACE): Mission Overview, *Geophys. Res. Lett.*, 32, L15S01, doi:10.1029/2005GL022386, 2005. [10888](#)
- Brown, L., Benner, D. C., Champion, J., Devi, V., Fejard, L., Gamache, R., Gabard, T., Hilico, J., Lavorel, B., Loete, M., Mellau, G., Nikitin, A., Pine, A., Predoi-Cross, A., Rinsland, C., Robert, O., Sams, R., Smith, M., Tashkun, S., and Tyuterev, V.: Methane line parameters in HITRAN, *J. Quant. Spectrosc. Radiat. Transfer*, 82, 219–238, 2003. [10898](#)
- Carli, B., Alpaslan, D., Carlotti, M., Castelli, E., Ceccherini, S., Dinelli, B. M., Dudhia, A., Flaud, J. M., Hoepfner, M., Jay, V., Magnani, L., Oelhaf, H., Payne, V., Piccolo, C., Prosperi, M., Raspollini, P., Remedios, J., Ridolfi, M., and Spang, R.: First results of MIPAS/ENVISAT with operational Level 2 code, *Adv. Space Res.*, 33, 1012–1019, 2004. [10889](#)
- Coffey, M. T., Goldman, A., Hannigan, J. W., Mankin, W. G., Schoenfeld, W. G., Rinsland, C. P., Bernardo, C., and Griffith, D. W. T.: Improved Vibration-Rotation (0-1) HBr Line Parameters for Validating High Resolution Infrared Atmospheric Spectra Measurements, *J. Quant. Spectrosc. Radiat. Transfer*, 60, 863–867, 1998. [10891](#)
- Dils, B., de Mazière, M., Müller, J. F., Blumenstock, T., Buchwitz, M., de Beek, R., Demoulin, P., Duchatelet, P., Fast, H., Frankenberg, C., Gloudemans, A., Griffith, D., Jones, N., Kerzenmacher, T., Kramer, I., Mahieu, E., Mellqvist, J., Mittermeier, R. L., Notholt, J., Rinsland, C. P., Schrijver, H., Smale, D., Strandberg, A., Straume, A. G., Stremme, W., Strong, K., Sussmann, R., Taylor, J., van den Broek, M., Velazco, V., Wagner, T., Warneke, T., Wiacek, A., and Wood, S.: Comparisons between SCIAMACHY and ground-based FTIR data for total columns of CO, CH<sub>4</sub>, CO<sub>2</sub> and N<sub>2</sub>O, *Atmos. Chem. Phys.*, 6, 1953–1976, 2006. [10886](#)

## Simultaneous Observations with Three FTSs

D. Wunch et al.

Title Page

Abstract

Introduction

Conclusions

References

Tables

Figures

◀

▶

◀

▶

Back

Close

Full Screen / Esc

Printer-friendly Version

Interactive Discussion

---

**Simultaneous  
Observations with  
Three FTSs**D. Wunch et al.

---

Title Page

Abstract

Introduction

Conclusions

References

Tables

Figures

◀

▶

◀

▶

Back

Close

Full Screen / Esc

Printer-friendly Version

Interactive Discussion

Fu, D., Walker, K. A., Sung, K., Boone, C. D., Soucy, M. A., and Bernath, P. F.: The portable atmospheric research interferometric spectrometer for the infrared, *PARIS-IR*, *J. Quant. Spectrosc. Radiat. Transfer*, 2006. [10888](#)

Gallery, W. O., Kneizys, F. X., and Clough, S. A.: Air mass computer program for atmospheric transmittance/radiance calculation: FSCATM, AFGL-TR-0208 Environmental Research papers, 1983. [10889](#)

Goldman, A., Paton-Walsh, C., Bell, W., Toon, G. C., Blavier, J.-F., Sen, B., Coffey, M. T., Hannigan, J. W., and Mankin, W. G.: Network for the Detection of Stratospheric Change Fourier transform infrared intercomparison at Table Mountain Facility, November 1996, *J. Geophys. Res.*, 104, 30 481–30 503, 1999. [10884](#), [10885](#), [10890](#), [10908](#)

Griffith, D. W. T., Jones, N. B., McNamara, B., Paton-Walsh, C., Bell, W., and Bernardo, C.: Intercomparison of NDSC ground-based solar FTIR measurements of atmospheric gases at Lauder, New Zealand, *J. Atmos. Ocean. Technol.*, 20, 1138–1153, 2003. [10884](#), [10885](#), [10890](#), [10895](#), [10908](#)

Hase, F., Blumenstock, T., and Paton-Walsh, C.: Analysis of the instrumental line shape of high-resolution Fourier transform IR spectrometers with gas cell measurements and new retrieval software, *Appl. Opt.*, 38, 3417–3422, 1999. [10891](#), [10909](#)

Hase, F., Hannigan, J., Coffey, M., Goldman, A., Höpfner, M., Jones, N., Rinsland, C., and Wood, S.: Intercomparison of retrieval codes used for the analysis of high-resolution, ground-based FTIR measurements, *J. Quant. Spectrosc. Radiat. Transfer*, 87, 25–52, 2004. [10884](#)

Kerzenmacher, T. E., Walker, K. A., Strong, K., Berman, R., Bernath, P. F., Boone, C. D., Drummond, J. R., Fast, H., Fraser, A., MacQuarrie, K., Midwinter, C., Sung, K., McElroy, C. T., Mittermeier, R. L., Walker, J., and Wu, H.: Measurements of O<sub>3</sub>, NO<sub>2</sub> and Temperature during the 2004 Canadian Arctic ACE Validation Campaign, *Geophys. Res. Lett.*, 32, L16S07, doi:10.1029/2005GL023032, 2005. [10888](#)

Kurylo, M. J. and Zander, R. J.: The NDSC – Its status after ten years of operation, in: Proceedings of XIX Quadrennial Ozone Symposium, Hokkaido University, Sapporo, Japan, pp. 167–168, 2000. [10885](#)

Mahieu, E., Zander, R., Duchatelet, P., Hannigan, J. W., Coffey, M. T., Mikuteit, S., Hase, F., Blumenstock, T., Wiacek, A., Strong, K., Taylor, J. R., Mittermeier, R., Fast, H., Boone, C. D., McLeod, S. D., Walker, K. A., Bernath, P. F., and Rinsland, C. P.: Comparisons between ACE-FTS and ground-based measurements of stratospheric HCl and ClONO<sub>2</sub> loadings at northern latitudes, *Geophys. Res. Lett.*, 32, L15S08, doi:10.1029/2005GL022396, 2005. [10886](#)

Meier, A., Goldman, A., Manning, P. S., Stephen, T. M., Rinsland, C. P., Jones, N. B., and Wood, S. W.: Improvements to air mass calculations for ground-based infrared measurements, *J. Quant. Spectrosc. Radiat. Transfer*, 83, 109–113, 2004. [10889](#)

Meier, A., Paton-Walsh, C., Bell, W., Blumenstock, T., Hase, F., Goldman, A., Steen, A., Kift, R., Woods, P., and Kondo, Y.: Evidence of reduced measurement uncertainties from an FTIR instrument intercomparison at Kiruna, Sweden, *J. Quant. Spectrosc. Radiat. Transfer*, 96, 75–84, 2005. [10884](#), [10885](#), [10898](#), [10908](#)

Paton-Walsh, C., Bell, W., Gardiner, T., Swann, N., Woods, P., Notholt, J., Schütt, H., Galle, B., Arlander, W., and Mellqvist, J.: An uncertainty budget for ground-based Fourier transform infrared column measurements of HCl, HF, N<sub>2</sub>O and HNO<sub>3</sub> deduced from results of side-by-side instrument intercomparisons, *J. Geophys. Res.*, 102, 8867–8873, 1997. [10884](#), [10885](#), [10908](#)

Pougatchev, N. S., Connor, B. J., and Rinsland, C. P.: Infrared measurements of the ozone vertical distribution above Kitt Peak, *J. Geophys. Res.*, 100, 16 689–16 698, doi:10.1029/95JD01296, 1995. [10889](#)

Rinsland, C. P., Smith, M. A. H., Rinsland, P. L., Goldman, A., Brault, J. W., and Stokes, G.: Ground-based infrared spectroscopic measurements of atmospheric hydrogen cyanide, *J. Geophys. Res.*, 87, 11 119–11 125, 1982. [10889](#)

Rinsland, C. P., Jones, N. B., Connor, B. J., Logan, J. A., Pougatchev, N. S., Goldman, A., Murcray, F. J., Stephen, T. M., Pine, A. S., Zander, R., Mahieu, E., and Demoulin, P.: Northern and southern hemisphere ground-based infrared spectroscopic measurements of tropospheric carbon monoxide and ethane, *J. Geophys. Res.*, 103, 197–218, doi: 10.1029/98JD02515, 1998. [10888](#)

Rodgers, C. D.: *Inverse Methods for Atmospheric Sounding: Theory and Practice*, vol. 2 of *Series on Atmospheric, Oceanic and Planetary Physics*, World Scientific Co. Pte. Ltd., 2000. [10889](#), [10898](#)

Rodgers, C. D. and Connor, B. J.: Intercomparison of remote sounding instruments, *J. Geophys. Res.*, 108, 4116, doi:10.1029/2002JD002299, 2003. [10898](#)

Rothman, L., Jacquemart, D., Barbe, A., Benner, D. C., Birk, M., Brown, L., Carleer, M., Jr., C. C., Chance, K., Coudert, L., Dana, V., Devi, V., Flaud, J.-M., Gamache, R., Goldman, A., Hartmann, J.-M., Jucks, K., Maki, A., Mandin, J.-Y., Massie, S., Orphal, J., Perrin, A., Rinsland, C., Smith, M., Tennyson, J., Tolchenov, R., Toth, R., Auwera, J. V., Varanasi, P., and Wagner, G.: The HITRAN 2004 molecular spectroscopic database, *J. Quant. Spectrosc.*

---

## Simultaneous Observations with Three FTs

D. Wunch et al.

---

[Title Page](#)[Abstract](#)[Introduction](#)[Conclusions](#)[References](#)[Tables](#)[Figures](#)[◀](#)[▶](#)[◀](#)[▶](#)[Back](#)[Close](#)[Full Screen / Esc](#)[Printer-friendly Version](#)[Interactive Discussion](#)

- Radiat. Transfer, 96, 139–204, 2005. [10889](#), [10898](#)
- Russell, J. M., Gordley, L. L., Deaver, L., Thompson, R., and Park, J. H.: An overview of the Halogen Occultation Experiment (HALOE) and preliminary results, *Adv. Space Res.*, 14, 9–13, 1994. [10889](#)
- 5 Schoeberl, M., Newman, P., Nagatani, R. N., and Lait, L.: Goddard Automailer – NASA Goddard Space Flight Center Code 916, [science@hyperion.gsfc.nasa.gov](mailto:science@hyperion.gsfc.nasa.gov). [10889](#)
- Strong, K., Bailak, G., Barton, D., Bassford, M., Blatherwick, R., Brown, S., Chartrand, D., Davies, J., Drummond, J., Fogal, P., Forsberg, E., Hall, R., Jofre, A., Kaminski, J., Kosters, J., Laurin, C., McConnell, J., Mcelroy, C., Menzies, K., Midwinter, C., Murcray, F., Olson, R.,  
10 Quine, B., Rochon, Y., Savastiouk, V., Solheim, B., Sommerfeldt, D., Ullberg, A., Werchohlad, S., and Wunch, D.: MANTRA – A balloon mission to study the odd-nitrogen budget of the stratosphere, *Atmos. Ocean*, 43, 283–299, 2005. [10885](#)
- Wiacek, A.: First Trace Gas Measurements Using Fourier Transform Infrared Solar Absorption Spectroscopy at the University of Toronto Atmospheric Observatory, Ph.D. thesis, University of Toronto, 2006. [10889](#)
- 15 Wiacek, A., Strong, K., Jones, N. B., Taylor, J. R., Mittermeier, R. L., and Fast, H.: First detection of meso-thermospheric Nitric Oxide (NO) by ground-based FTIR solar absorption spectroscopy, *Geophys. Res. Lett.*, 33, doi:10.1029/2005GL024897, 2006. [10886](#)
- Wiacek, A., Taylor, J. R., Strong, K., Saari, R., Kerzenmacher, T. E., Jones, N. B., and Griffith, D. W. T.: Ground-based solar absorption FTIR spectroscopy: a novel optical design instrument at a new NDSC Complementary Station, characterization of retrievals and first results, *J. Atmos. Ocean. Technol.*, in press, 2006. [10886](#), [10889](#)
- 20 Worden, J., Kulawik, S. S., Shephard, M. W., Clough, S. A., Worden, H., Bowman, K., and Goldman, A.: Predicted errors of tropospheric emission spectrometer nadir retrievals from spectral window selection, *J. Geophys. Res.*, 109, 9308, doi:10.1029/2004JD004522, 2004. [10898](#)
- 25 Wunch, D., Midwinter, C., Drummond, J. R., McElroy, C. T., and Bagès, A.-F.: The University of Toronto's Balloon-Borne Fourier Transform Spectrometer, *Rev. Sci. Inst.*, 77, 093104-1–093104-7, 2006. [10887](#)

---

**Simultaneous  
Observations with  
Three FTs**D. Wunch et al.

---

Title Page

Abstract

Introduction

Conclusions

References

Tables

Figures

◀

▶

◀

▶

Back

Close

Full Screen / Esc

Printer-friendly Version

Interactive Discussion

## Simultaneous Observations with Three FTSs

D. Wunch et al.

**Table 1.** Instrument configuration. The second line of the spectral range for the TAO-FTS indicates its spectral range using NDACC filter 3, which is the spectral range used in this inter-comparison. The scan time is the time it takes to record a single interferogram.

	PARIS-IR	U of T FTS	TAO-FTS
Maximum OPD (cm)	25	50	250
Scan time (s)	20	50	300
Spectral range (cm <sup>-1</sup> )	750–4400	1200–5000	750–4400 2400–3100
Measurement dates	24 Aug.–2 Sept.	26 May–12 Sept.	Year-round

Title Page

Abstract

Introduction

Conclusions

References

Tables

Figures

◀

▶

◀

▶

Back

Close

Full Screen / Esc

Printer-friendly Version

Interactive Discussion

## Simultaneous Observations with Three FTSs

D. Wunch et al.

**Table 2.** Microwindows for O<sub>3</sub>, HCl, N<sub>2</sub>O and CH<sub>4</sub> used in this intercomparison. The 2775 O<sub>3</sub> and CH<sub>4</sub> microwindows each consist of three separate bandpasses retrieved simultaneously. The names of the individual bandpasses are in brackets.

Target Gas	Microwindow	Spectral Range (cm <sup>-1</sup> )	Interfering Species
O <sub>3</sub>	3040	3039.90–3040.60	H <sub>2</sub> O, CH <sub>4</sub>
O <sub>3</sub>	(2775)	2775.68–2776.30	CH <sub>4</sub> , CO <sub>2</sub> , HCl, N <sub>2</sub> O
	(2778)	2778.85–2779.20	CH <sub>4</sub> , HDO, N <sub>2</sub> O
	(2782)	2781.57–2782.06	CH <sub>4</sub> , HDO, N <sub>2</sub> O, CO <sub>2</sub>
HCl	2925	2925.75–2926.05	H <sub>2</sub> O, CH <sub>4</sub> , N <sub>2</sub> O, O <sub>3</sub>
N <sub>2</sub> O	2482	2481.30–2482.60	CO <sub>2</sub> , CH <sub>4</sub> , O <sub>3</sub>
CH <sub>4</sub>	(2859)	2859.83–2860.21	–
	(2898)	2898.32–2898.98	–
	(2904)	2903.60–2904.16	H <sub>2</sub> O, HCl, O <sub>3</sub>

[Title Page](#)
[Abstract](#)
[Introduction](#)
[Conclusions](#)
[References](#)
[Tables](#)
[Figures](#)
[Back](#)
[Close](#)
[Full Screen / Esc](#)
[Printer-friendly Version](#)
[Interactive Discussion](#)

## Simultaneous Observations with Three FTSs

D. Wunch et al.

**Table 3.** Microwindow degrees of freedom for signal and fitting parameters for O<sub>3</sub>, HCl, N<sub>2</sub>O and CH<sub>4</sub>. The mean degrees of freedom for signal were obtained from retrievals performed using the retrieval parameters listed in the last three columns. SPHS is the simple phase parameter. PHS and EAP are the third order phase and effective apodization polynomial coefficients. For the U of T FTS, they are retrieved directly from the microwindow itself. For PARIS-IR, they are retrieved from a nearby broad-band N<sub>2</sub>O microwindow.

Target Gas	Microwindow	Degrees of Freedom for Signal			Retrieved ILS Parameters		
		TAO	U of T	PARIS-IR	TAO	U of T	PARIS-IR
O <sub>3</sub>	3040	2.4	1.32	1.03	SPHS	SPHS, PHS, EAP	SPHS, PHS, EAP
O <sub>3</sub>	2775	2.1	1.35	0.83	SPHS	SPHS, PHS, EAP	SPHS, PHS, EAP
HCl	2925	3.1	1.23	0.67	SPHS	SPHS, PHS, EAP	SPHS, PHS, EAP
N <sub>2</sub> O	2482	4.2	2.85	2.31	SPHS	SPHS, PHS, EAP	SPHS
CH <sub>4</sub>	2859	4.0	2.68	2.38	SPHS	SPHS	SPHS

Title Page

Abstract

Introduction

Conclusions

References

Tables

Figures

◀

▶

◀

▶

Back

Close

Full Screen / Esc

Printer-friendly Version

Interactive Discussion

## Simultaneous Observations with Three FTSs

D. Wunch et al.

**Table 4.** Percent differences of mean total column values from Figs. 13–17 and results from previous intercomparisons. Bold PARIS-IR and U of T FTS differences indicate that they are significant to 95% by the Student's t-test (i.e.  $t \geq 1.96$ ). The PARIS-IR and U of T FTS percent differences are from the TAO-FTS, for SZA >40 degrees. For the previous intercomparisons, brackets beneath the percent differences for each molecule indicate the microwindow retrieved, if it is different from Table 2. Here, for the Meier et al. (2005), Griffith et al. (2003), and Paton-Walsh et al. (1997) papers, we cite mean percent differences between the two instruments over the duration of the intercomparison, whereas for Goldman et al. (1999), we cite the maximum difference from the average of the three instruments involved for the November 11B data set.

	3040	O <sub>3</sub> 2775	HCl 2925	N <sub>2</sub> O 2482	CH <sub>4</sub> 2859
PARIS-IR percent difference from TAO	0.8	<b>2.6</b>	<b>3.2</b>	0.4	0.5
U of T FTS percent difference from TAO	<b>3.3</b>	0.7	1.7	0.4	<b>2.3</b>
U of T FTS percent difference from PARIS-IR	<b>2.5</b>	<b>3.2</b>	1.5	0.8	<b>1.7</b>
Meier et al. (2005)		0.4 (3040)	0.7	0.1	0.2 (2904)
Griffith et al. (2003)		2.57 (3045.08–3045.38)	2.90	0.34	1.11 (2904)
Goldman et al. (1999)		1.5 (3045.08–3045.38)	1.6	1.1	0.2 (2904)
Paton-Walsh et al. (1997)		N/A	0.5	1.0	N/A

Title Page

Abstract

Introduction

Conclusions

References

Tables

Figures

◀

▶

◀

▶

Back

Close

Full Screen / Esc

Printer-friendly Version

Interactive Discussion

**Simultaneous  
Observations with  
Three FTSs**

D. Wunch et al.

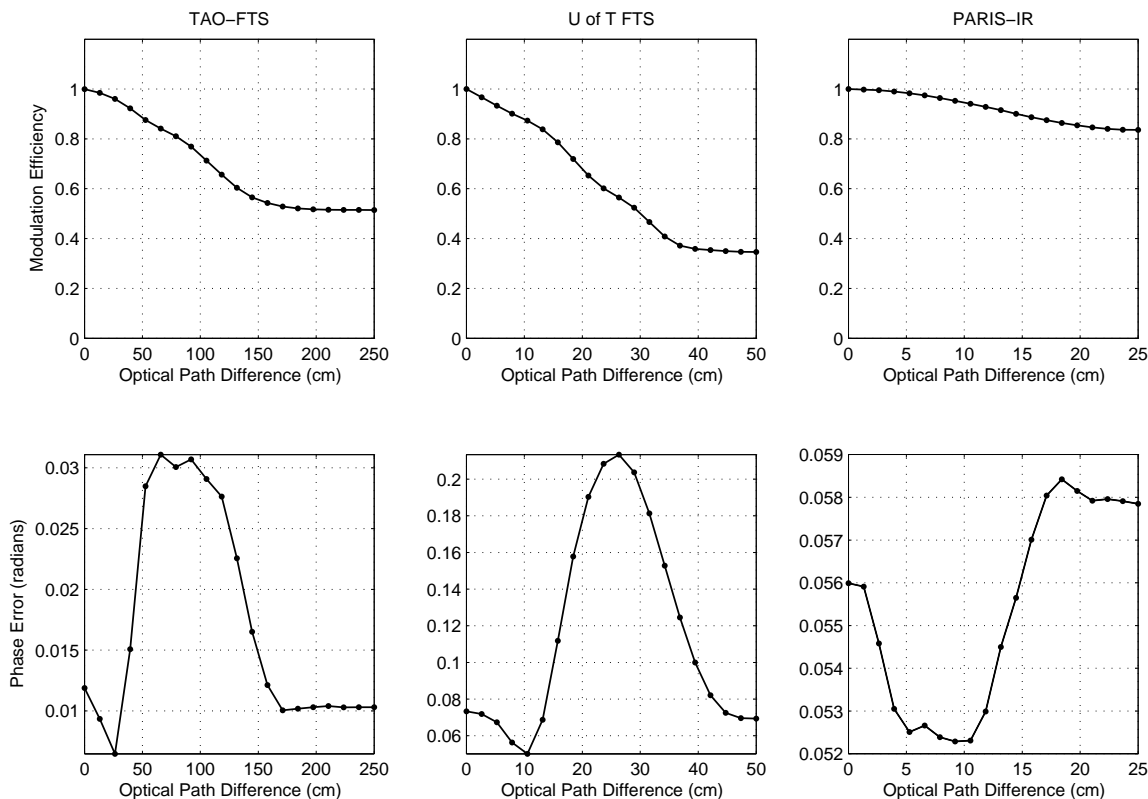


**Fig. 1.** Typical modulation efficiency and phase error for all three instruments. These are computed from gas cell measurements using the LINEFIT software (Hase et al., 1999). The top panels contain the modulation efficiency and the lower panels contain the phase error. The left-most panels show unapodized TAO-FTS data, recorded in August, 2005. The central panels show U of T FTS data, apodized with a triangular filter and recorded in September, 2005. The right-most panels show unapodized PARIS-IR data, recorded in August, 2005.

Title Page

Abstract

Introduction

Conclusions

References

Tables

Figures

◀

▶

◀

▶

Back

Close

Full Screen / Esc

Printer-friendly Version

Interactive Discussion

## Simultaneous Observations with Three FTSs

D. Wunch et al.

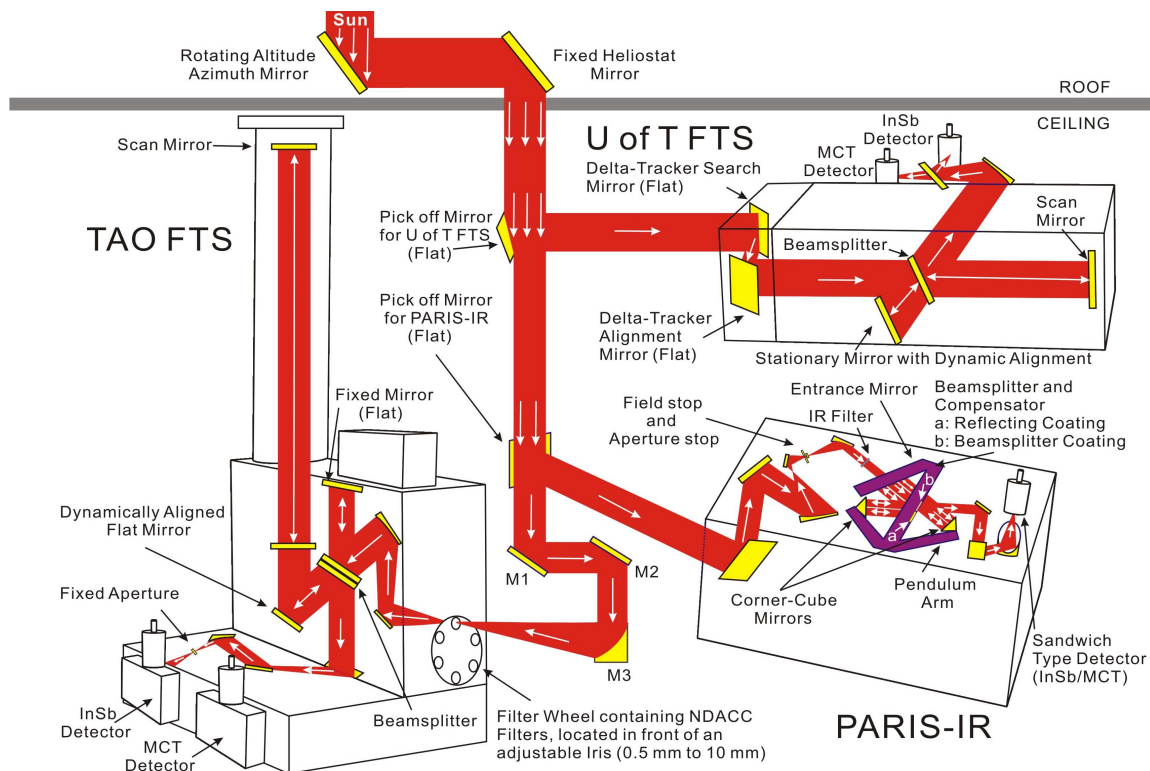


**Fig. 2.** The experimental setup.

Title Page

Abstract

Introduction

Conclusions

References

Tables

Figures

◀

▶

◀

▶

Back

Close

Full Screen / Esc

Printer-friendly Version

Interactive Discussion

Simultaneous  
Observations with  
Three FTs

D. Wunch et al.

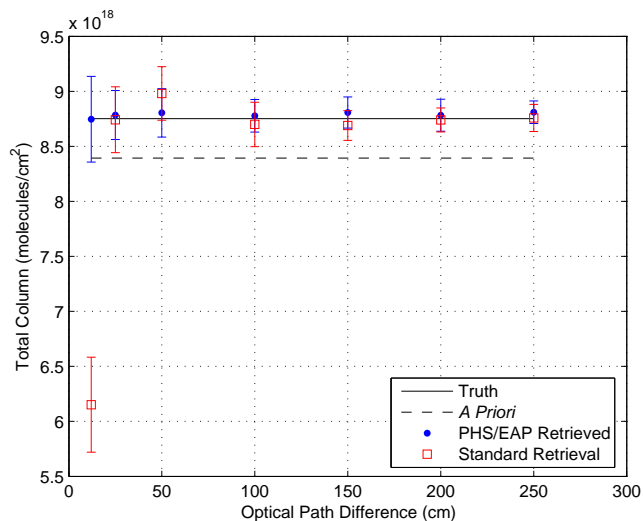


**Fig. 3.** Simulated retrievals of ozone columns in the  $3040\text{ cm}^{-1}$  microwindow, assuming  $\text{SNR}=250$ , as a function of OPD.

[Title Page](#)[Abstract](#)[Introduction](#)[Conclusions](#)[References](#)[Tables](#)[Figures](#)[◀](#)[▶](#)[◀](#)[▶](#)[Back](#)[Close](#)[Full Screen / Esc](#)[Printer-friendly Version](#)[Interactive Discussion](#)

**Simultaneous  
Observations with  
Three FTs**

D. Wunch et al.

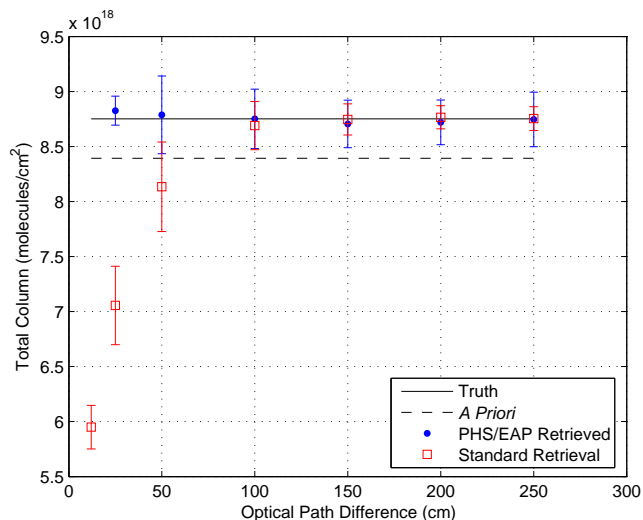


**Fig. 4.** Simulated retrievals of ozone columns in the  $2775\text{ cm}^{-1}$  microwindow, assuming  $\text{SNR}=250$ , as a function of OPD. The small error bars on the PHS/EAP retrieval for 25 cm OPD are due to the small number of retrievals that converged for this OPD. The error bars are, as a consequence, artificially small.

[Title Page](#)[Abstract](#)[Introduction](#)[Conclusions](#)[References](#)[Tables](#)[Figures](#)[◀](#)[▶](#)[◀](#)[▶](#)[Back](#)[Close](#)[Full Screen / Esc](#)[Printer-friendly Version](#)[Interactive Discussion](#)

**Simultaneous  
Observations with  
Three FTs**

D. Wunch et al.

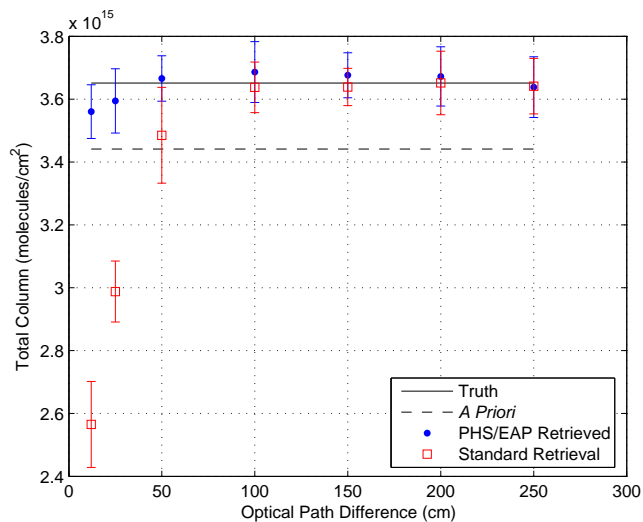


**Fig. 5.** Simulated retrievals of HCl columns, assuming SNR=250, as a function of OPD.

[Title Page](#)[Abstract](#)[Introduction](#)[Conclusions](#)[References](#)[Tables](#)[Figures](#)[◀](#)[▶](#)[◀](#)[▶](#)[Back](#)[Close](#)[Full Screen / Esc](#)[Printer-friendly Version](#)[Interactive Discussion](#)

**Simultaneous  
Observations with  
Three FTs**

D. Wunch et al.

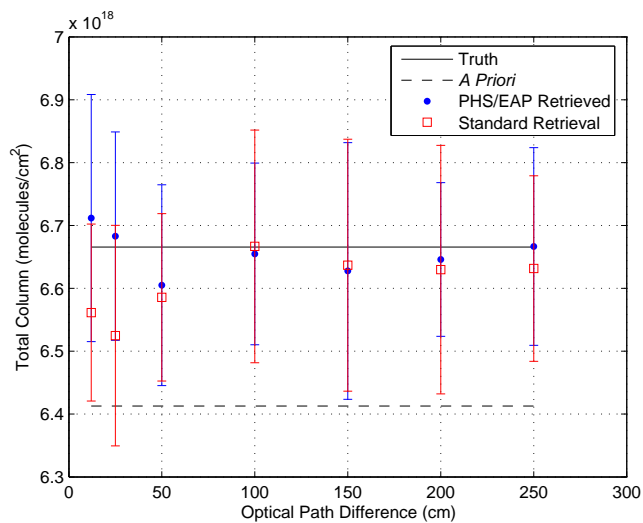


**Fig. 6.** Simulated retrievals of N<sub>2</sub>O columns, assuming SNR=250, as a function of OPD.

[Title Page](#)[Abstract](#)[Introduction](#)[Conclusions](#)[References](#)[Tables](#)[Figures](#)[◀](#)[▶](#)[◀](#)[▶](#)[Back](#)[Close](#)[Full Screen / Esc](#)[Printer-friendly Version](#)[Interactive Discussion](#)

**Simultaneous  
Observations with  
Three FTs**

D. Wunch et al.

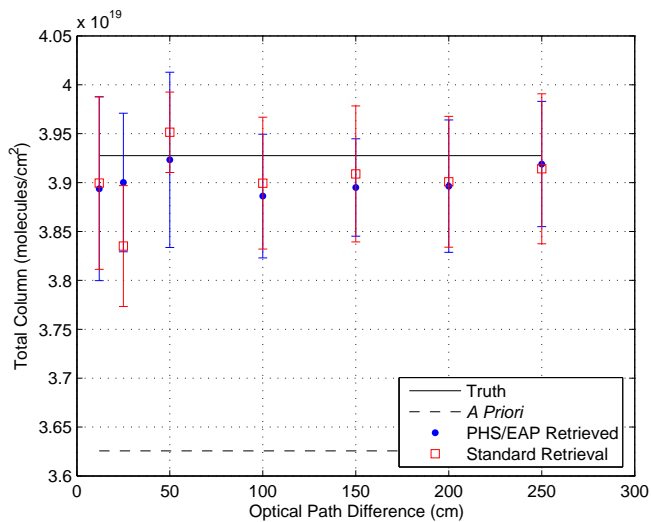


**Fig. 7.** Simulated retrievals of CH<sub>4</sub> columns, assuming SNR=250, as a function of OPD.

[Title Page](#)[Abstract](#)[Introduction](#)[Conclusions](#)[References](#)[Tables](#)[Figures](#)[⏪](#)[⏩](#)[◀](#)[▶](#)[Back](#)[Close](#)[Full Screen / Esc](#)[Printer-friendly Version](#)[Interactive Discussion](#)

## Simultaneous Observations with Three FTs

D. Wunch et al.

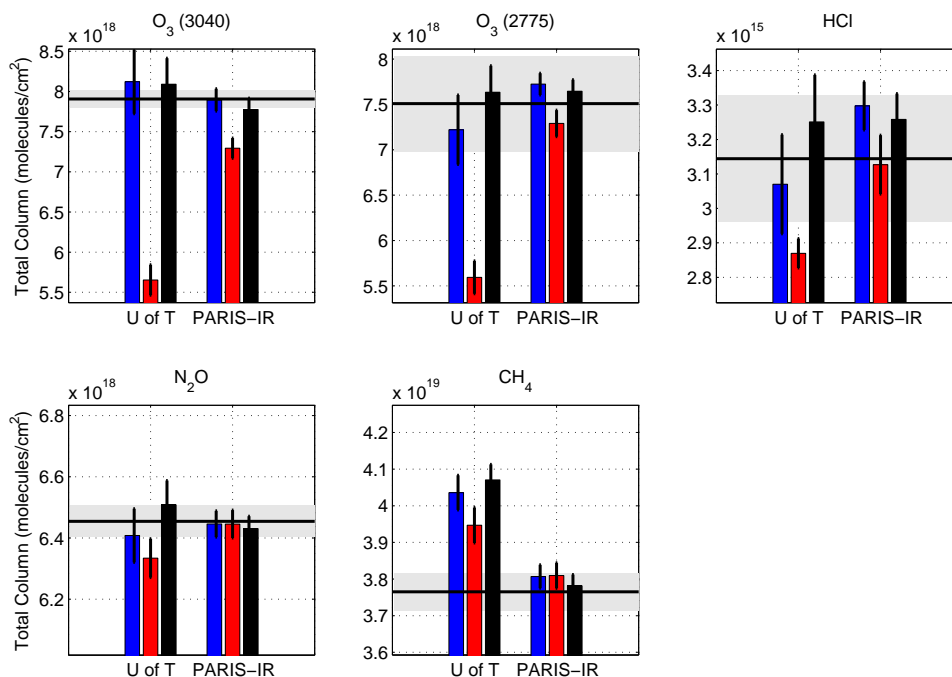


**Fig. 8.** Mean column differences from data recorded on 2 September, using the PHS/EAP retrieval (blue), the standard retrieval (red) and the ILS input retrieval (black). The thick black horizontal line indicates the TAO-FTS mean and the grey shading is the standard deviation of the TAO-FTS retrieved values. The error bars on the bars indicate the standard deviation of the retrieved values.

[Title Page](#)
[Abstract](#)
[Introduction](#)
[Conclusions](#)
[References](#)
[Tables](#)
[Figures](#)
[◀](#)
[▶](#)
[◀](#)
[▶](#)
[Back](#)
[Close](#)
[Full Screen / Esc](#)
[Printer-friendly Version](#)
[Interactive Discussion](#)

**Simultaneous  
Observations with  
Three FTSs**

D. Wunch et al.

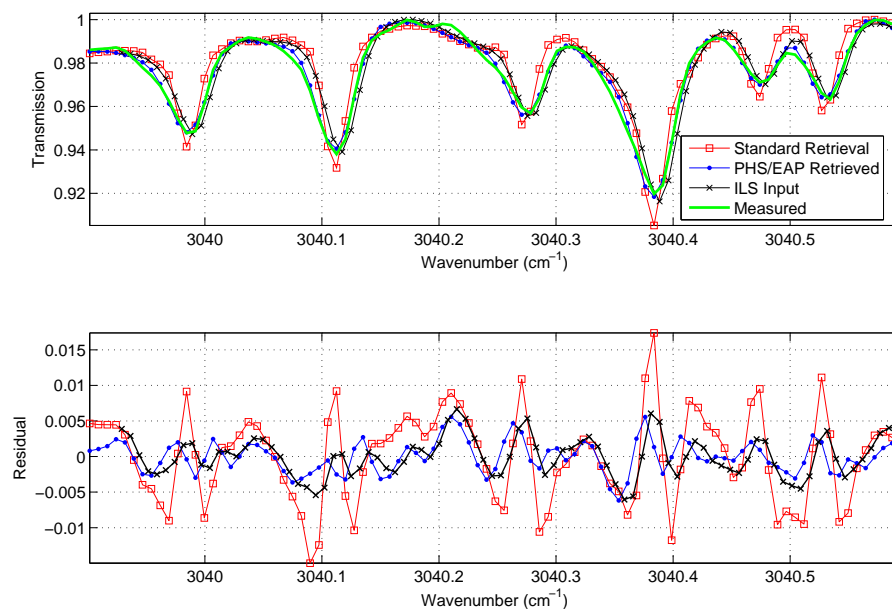


**Fig. 9.**  $\text{O}_3$  (3040) spectral fits for the U of T FTS (upper panel), and the residuals between the measured retrieval and the spectral fits (lower panel).

[Title Page](#)[Abstract](#)[Introduction](#)[Conclusions](#)[References](#)[Tables](#)[Figures](#)[◀](#)[▶](#)[◀](#)[▶](#)[Back](#)[Close](#)[Full Screen / Esc](#)[Printer-friendly Version](#)[Interactive Discussion](#)

Simultaneous  
Observations with  
Three FTSs

D. Wunch et al.

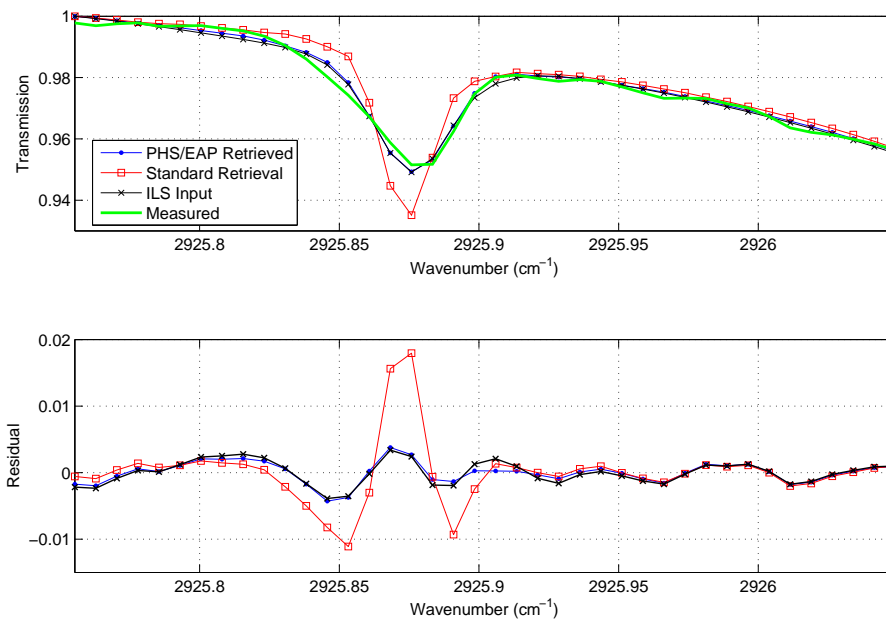


**Fig. 10.** HCl spectral fits for the U of T FTS (upper panel), and the corresponding residuals (lower panel).

[Title Page](#)[Abstract](#)[Introduction](#)[Conclusions](#)[References](#)[Tables](#)[Figures](#)[◀](#)[▶](#)[◀](#)[▶](#)[Back](#)[Close](#)[Full Screen / Esc](#)[Printer-friendly Version](#)[Interactive Discussion](#)

**Simultaneous  
Observations with  
Three FTs**

D. Wunch et al.

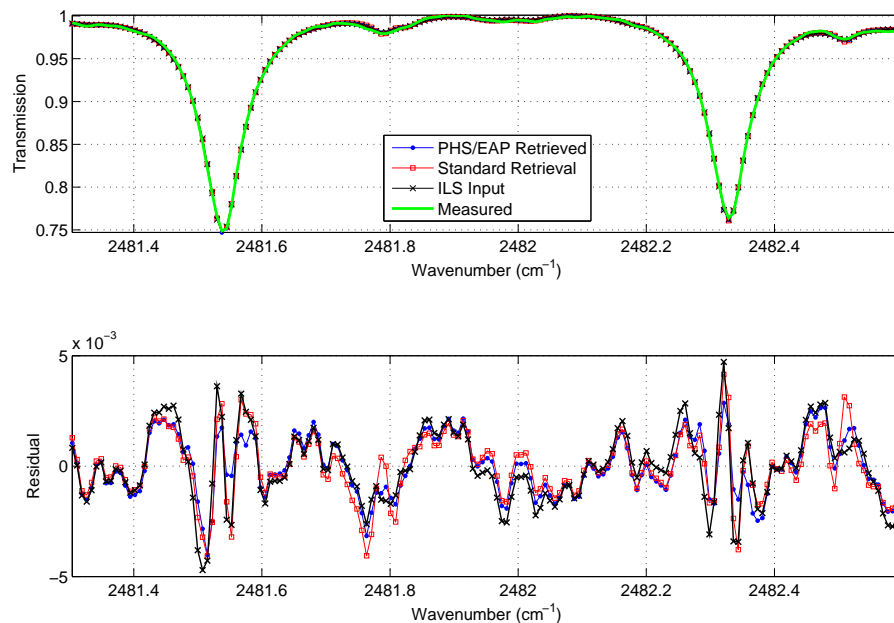


**Fig. 11.** N<sub>2</sub>O spectral fits for the U of T FTS (upper panel), and the corresponding residuals (lower panel).

[Title Page](#)[Abstract](#)[Introduction](#)[Conclusions](#)[References](#)[Tables](#)[Figures](#)[◀](#)[▶](#)[◀](#)[▶](#)[Back](#)[Close](#)[Full Screen / Esc](#)[Printer-friendly Version](#)[Interactive Discussion](#)

Simultaneous  
Observations with  
Three FTSs

D. Wunch et al.

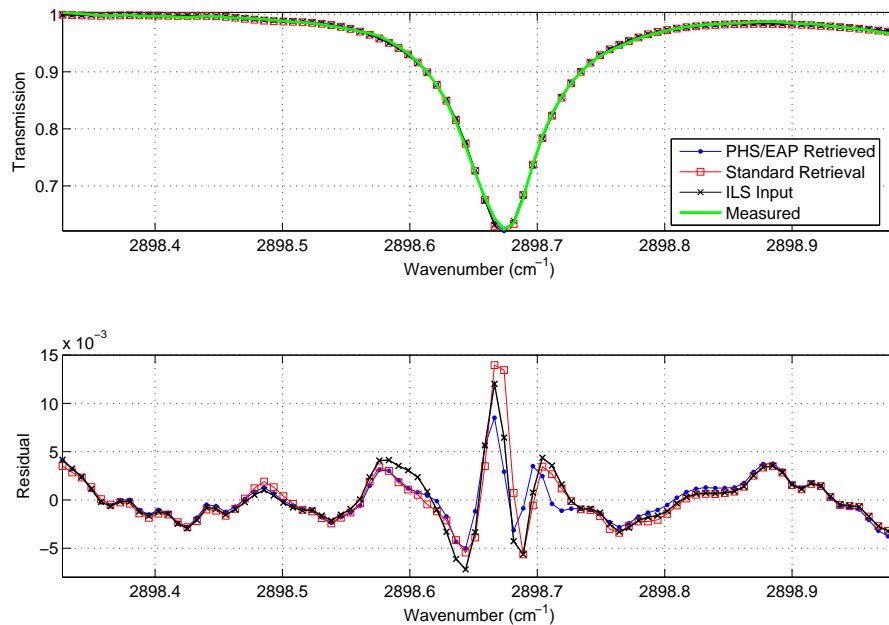


**Fig. 12.**  $\text{CH}_4$  spectral fits for the U of T FTS (upper panel), and the corresponding residuals (lower panel).

[Title Page](#)[Abstract](#)[Introduction](#)[Conclusions](#)[References](#)[Tables](#)[Figures](#)[◀](#)[▶](#)[◀](#)[▶](#)[Back](#)[Close](#)[Full Screen / Esc](#)[Printer-friendly Version](#)[Interactive Discussion](#)

Simultaneous  
Observations with  
Three FTSs

D. Wunch et al.

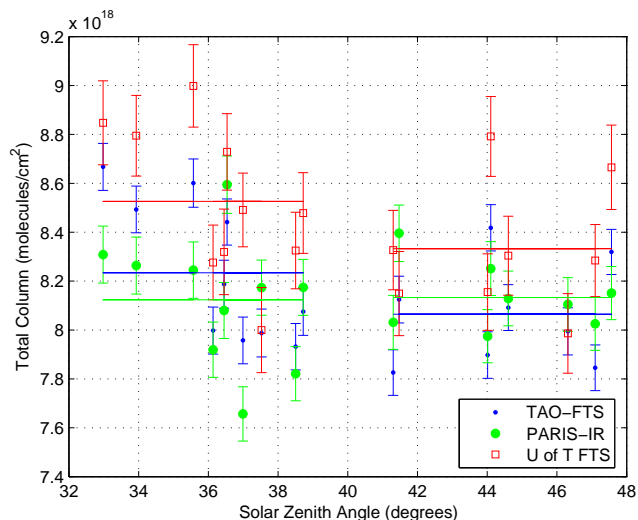


**Fig. 13.**  $\text{O}_3$  column amounts retrieved in the  $3040\text{ cm}^{-1}$  microwindow as a function of solar zenith angle, using the parameters described in Table 3. The horizontal lines show the means of the columns over the SZA range indicated. The error bars shown include the smoothing error, interference error and retrieval error added in quadrature.

[Title Page](#)[Abstract](#)[Introduction](#)[Conclusions](#)[References](#)[Tables](#)[Figures](#)[◀](#)[▶](#)[◀](#)[▶](#)[Back](#)[Close](#)[Full Screen / Esc](#)[Printer-friendly Version](#)[Interactive Discussion](#)

**Simultaneous  
Observations with  
Three FTSs**

D. Wunch et al.

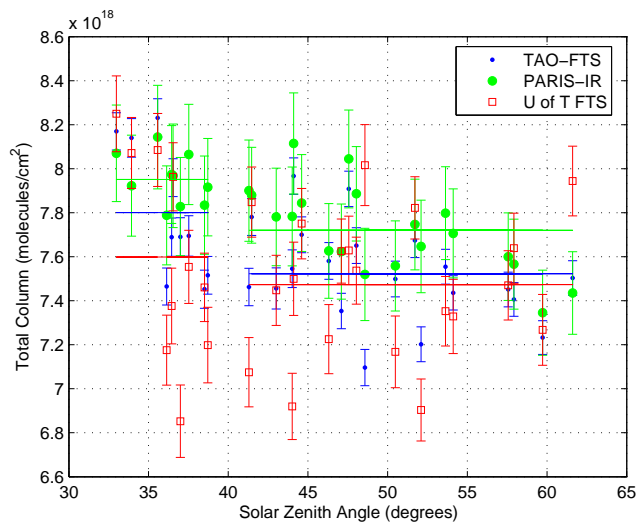


**Fig. 14.** As in Fig. 13, but for  $O_3$  in the  $2775\text{ cm}^{-1}$  microwindow.

Title Page

Abstract

Introduction

Conclusions

References

Tables

Figures

◀

▶

◀

▶

Back

Close

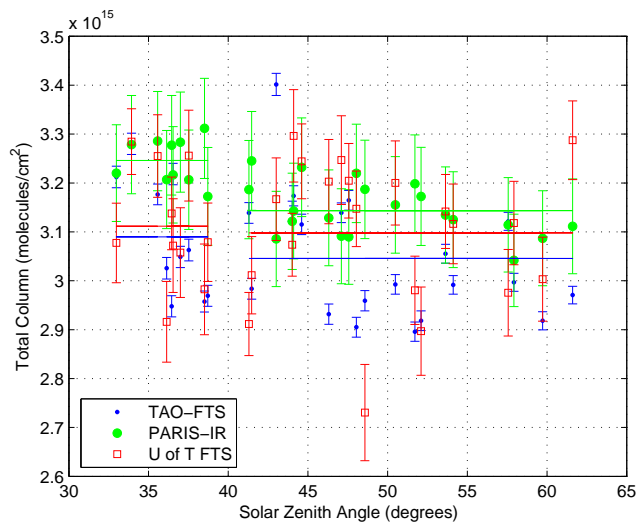
Full Screen / Esc

Printer-friendly Version

Interactive Discussion

**Simultaneous  
Observations with  
Three FTSs**

D. Wunch et al.

**Fig. 15.** As in Fig. 13, but for HCl.

Title Page

Abstract

Introduction

Conclusions

References

Tables

Figures

◀

▶

◀

▶

Back

Close

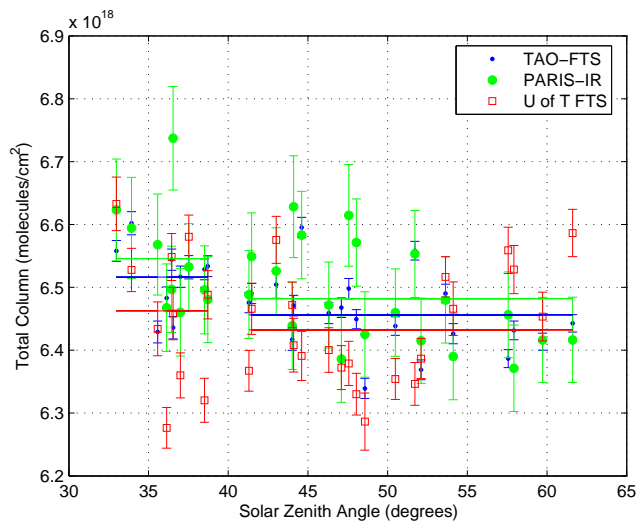
Full Screen / Esc

Printer-friendly Version

Interactive Discussion

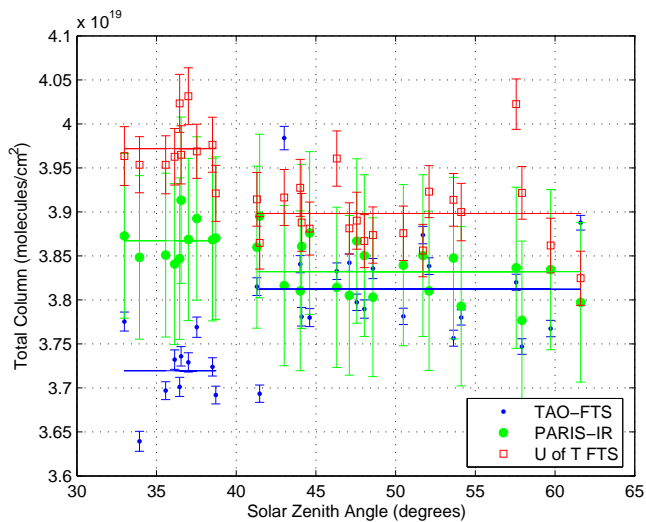
**Simultaneous  
Observations with  
Three FTSs**

D. Wunch et al.

**Fig. 16.** As in Fig. 13, but for  $N_2O$ .[Title Page](#)[Abstract](#)[Introduction](#)[Conclusions](#)[References](#)[Tables](#)[Figures](#)[⏪](#)[⏩](#)[◀](#)[▶](#)[Back](#)[Close](#)[Full Screen / Esc](#)[Printer-friendly Version](#)[Interactive Discussion](#)

**Simultaneous  
Observations with  
Three FTs**

D. Wunch et al.

**Fig. 17.** As in Fig. 13, but for CH<sub>4</sub>.[Title Page](#)[Abstract](#)[Introduction](#)[Conclusions](#)[References](#)[Tables](#)[Figures](#)[◀](#)[▶](#)[◀](#)[▶](#)[Back](#)[Close](#)[Full Screen / Esc](#)[Printer-friendly Version](#)[Interactive Discussion](#)

**Simultaneous  
Observations with  
Three FTs**

D. Wunch et al.

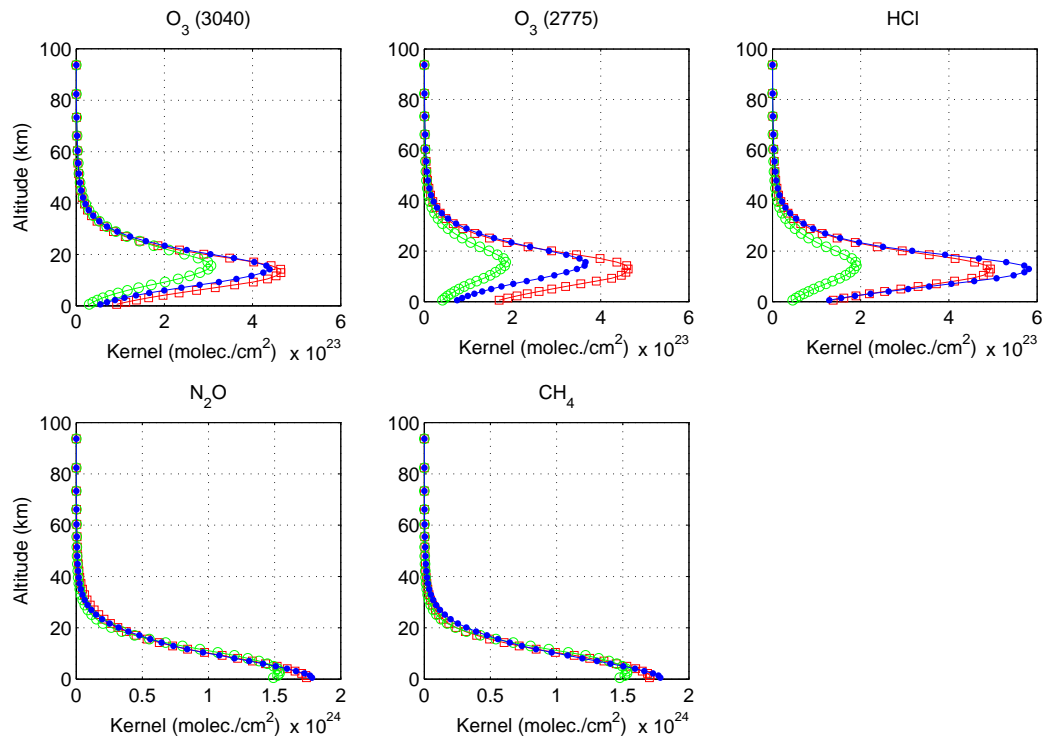


**Fig. 18.** Density-weighted column averaging kernels for the three instruments: TAO (blue dots), U of T FTs (red squares) and PARIS-IR (green circles), illustrating the sensitivity of the retrieved column at each altitude.

[Title Page](#)[Abstract](#)[Introduction](#)[Conclusions](#)[References](#)[Tables](#)[Figures](#)[◀](#)[▶](#)[◀](#)[▶](#)[Back](#)[Close](#)[Full Screen / Esc](#)[Printer-friendly Version](#)[Interactive Discussion](#)

**Simultaneous  
Observations with  
Three FTs**

D. Wunch et al.

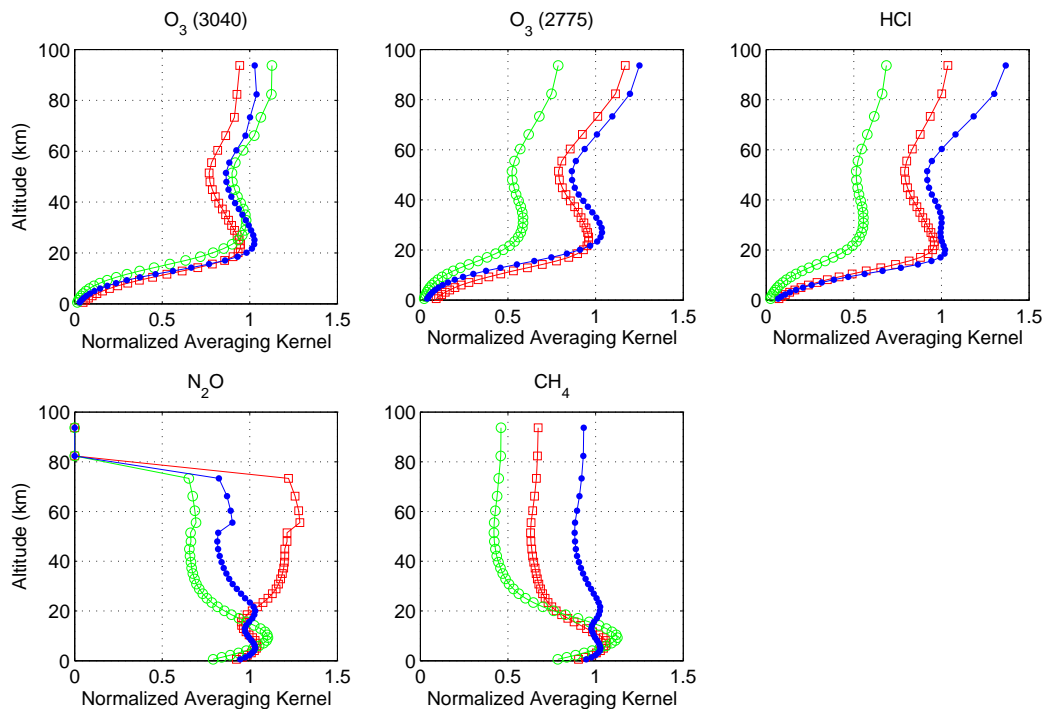


**Fig. 19.** Normalized column averaging kernels. These panels show the normalized column averaging kernels for for the three instruments: TAO (blue dots), U of T FTS (red squares) and the PARIS-IR (green circles).

[Title Page](#)[Abstract](#)[Introduction](#)[Conclusions](#)[References](#)[Tables](#)[Figures](#)[◀](#)[▶](#)[◀](#)[▶](#)[Back](#)[Close](#)[Full Screen / Esc](#)[Printer-friendly Version](#)[Interactive Discussion](#)

## Simultaneous Observations with Three FTs

D. Wunch et al.

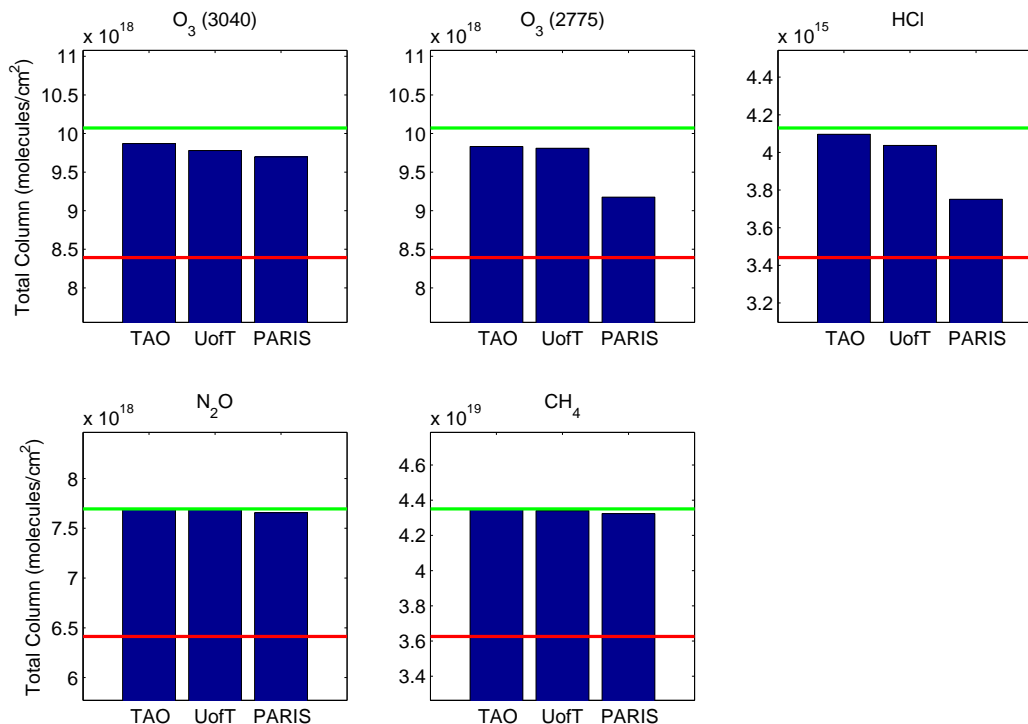


**Fig. 20.** Total columns derived by applying the averaging kernels to a profile that is the a priori profile increased by 20% at each layer. The red lines indicate the a priori column amount and the green lines indicate the a priori column amount, increased by 20% (the “true” column value, in this case).

Title Page

Abstract

Introduction

Conclusions

References

Tables

Figures

◀

▶

◀

▶

Back

Close

Full Screen / Esc

Printer-friendly Version

Interactive Discussion